

## Activity sources from fast large-scale brain recordings in adult *Drosophila*

Sophie Aimon<sup>1,\*</sup>, Takeo Katsuki<sup>1</sup>, Logan Grosenick<sup>2</sup>, Michael Broxton<sup>2</sup>, Karl Deisseroth<sup>2</sup>, Ralph Greenspan<sup>1</sup>

1. Kavli Institute for Brain and Mind, UCSD, La Jolla, CA 92093-0126, USA

2. Departments of Computer Science and Bioengineering, Stanford University, Stanford, CA 94305, USA

\*To whom correspondence should be addressed: [saimon@ucsd.edu](mailto:saimon@ucsd.edu)

### Abstract

We provide a method to record near-whole brain activity in behaving adult flies and extract signals from specific anatomical structures. We image pan-neuronal calcium or voltage sensors fluorescence at high speed with light field microscopy. We then apply computational methods to extract functional maps, and find that their characteristic shape match the anatomy of sub-neuropile regions and sometimes small population of neurons. Associated time series are also consistent with the literature.

Measuring activity at the scale of the brain is essential for understanding how different regions interact to process sensory information, control internal states, and generate behaviors. However techniques for imaging a whole brain so far have been orders of magnitude slower than the fastest neuronal electrical activity—a recent report of whole brain fluorescence imaging in *Drosophila* larvae had a frame rate of 5 Hz<sup>1</sup>. A newly developed technique, light field microscopy<sup>2-5</sup>, makes it possible to image large volumes at the frame rate of the fastest sCMOS cameras.

Here, we leverage this technique to record large scale activity in the adult fruit fly brain. We first show that the whole brain can be imaged with a 20x objective at a frame rate up to 200 Hz. We record the fluorescence of a pan-neuronally expressed calcium (GCaMP6f<sup>6</sup>) or voltage (Arclight<sup>7</sup>) probe. We apply computational methods (principal component analysis: PCA, and independent component analysis: ICA) to extract components representing spatially distinct sources of activity<sup>5,8,9</sup>. We show that these sources correspond to sub-neuropile areas or processes from small populations of neurons well defined anatomically, while their response to flashes of light or odor puffs is consistent with the literature.

We prepared a fly so as to fix its head and expose its brain while maintaining the eyes, antennae and legs clean (Supplementary Fig. 1). A ball was placed under its tarsi so that it could typically walk, groom, or rest. We imaged the fly brain fluorescence using light field microscopy: as shown in Figure 1a, an upright epifluorescence microscope (equipped with a 20x NA=1.0 objective) was modified by adding a microlens array at the image plane of the objective, and placing the camera sensor at the image plane of the microlens array through relay lenses<sup>4</sup>. We recorded light field images continuously with a high speed sCMOS camera at 100 Hz for GCaMP6f, or at 200 Hz using half the camera frame for Arclight. We then reconstructed the volumes—typically 600 x 300 x 200  $\mu\text{m}^3$  to encompass the whole brain (see Fig. 1b)—using the 3D deconvolution method for light field microscopy described in<sup>2</sup>. With 2 microns fluorescent beads embedded in a gel, we measured the point spread function and found that it widens with distance to the focal plane, varying from 3.5 to 12  $\mu\text{m}$  laterally and from 6 to 35  $\mu\text{m}$  axially (Supplementary Fig.1). As shown below, this resolution was sufficient to extract activity from sub-neuropile compartments.

We applied statistical techniques: PCA and ICA, to extract maps and time series of spatially distinct sources of activity. We inspected the result in an interactive ipython-notebook to separate components likely due to brain activity from components likely due to movement or noise. Figure 2a shows a z-stack containing all the putative activity related maps (z-score>2) from a pan-neuronal GCaMP6f recording. Different colors correspond to different components.

Even though PCA and ICA are mathematical algorithms using no prior information about the brain, most maps match well anatomical structures. In Figure 2b, left column presents a choice of maps from Figure 2a, Supplementary Figure 2a or Supplementary Figure 2b, while right column presents central complex structures from<sup>10</sup> or neuronal processes from<sup>11</sup> assembled using Virtual Fly Brain<sup>12</sup>. Several sub-neuropile regions are recognizable from the shape of the maps (e.g protocerebral bridge glomeruli, ellipsoid body rings, fan-shaped body layers and medulla columns). In some cases, a neuron type can be identified from the combination of sub-neuropile regions. For example, z-scored maps containing signal in one antennal lobe glomerulus, in the calyx, and in the lateral horn, likely arise from the activity of one type of antennal lobe projection neurons, while z-scored maps with signal spanning both the horizontal and the vertical mushroom body lobes likely arise from activity in alpha-beta or alpha'-beta' Kenyon cells. Bottom of Figure 2c shows an example of components obtained when using a more restrictive

driver: TH-Gal4 (see also Supplementary Figure 2b). The maps match well processes of dopaminergic PPL1 neurons innervating mushroom body alpha lobe compartments, each component thus corresponding to only one or two cells per hemisphere<sup>13</sup>. Voltage recordings with Arclight also give rise to maps portraying specific neuropiles (e.g. medulla columns, antennal lobe, calix, lateral horn, fan-shaped body layers, noduli and protocerebral bridge in Fig. 2d).

The time series are consistent with the literature. For example, the components that likely represent antennal lobe projection neurons are spontaneously active in the absence of odor but their activity strongly increases in response to odor puffs (Fig. 2d, Sup. Fig. 2a)<sup>14</sup>. Components in the optic lobe (medulla columns for example) respond to onset and/or offset of light (Fig. 2c and 2d, Sup. Fig. 3)<sup>15</sup>. With Arclight, the method permits the capturing of both graded potentials—e.g. components in the optic lobe in response to the flashes of light, and spikes—e.g. components in the antennal lobe, calix and lateral horn. The number of components with activity apparently unrelated with the stimuli varied from fly to fly, sometimes displaying strong oscillations (See Supplementary Fig. 3). Note that the ability to record membrane voltage signals in the actual neuronal processes performing the computation is an advantage over patch clamp experiments, as in the *Drosophila* brain the neuron on which patch clamp is performed is on the outside of the brain, and can be poorly representative of the activity in the neuronal processes<sup>16</sup>.

Although a black tape protects the fly's eyes from direct illumination by the microscope excitation light, the eye's blue receptors can still be activated by light scattered by the brain, as attested by the transient activity in the first few seconds of each experiment (data not shown). We presented flashes of blue light as stimuli to verify these receptors were not saturated. Although the stimulus excited fluorophores non-specifically, PCA and ICA could extract clear neuronal calcium responses in the optic lobes and the protocerebral bridge (Supplementary Fig. 4), thus demonstrating that the fly can still perceive external blue stimuli.

Applying PCA and ICA to large scale recordings of adult fly brain activity allows identifying some sub-neuropiles regions and sometimes neuron types responding to flashes of light or odors. This technique could thus be used as a functional screen to identify brain regions and neurons involved in processing any stimulus or behavior that can be performed under the microscope (see possible limitations in Supplementary Note). Furthermore, contrary to screens using activation or silencing of specific neurons, the components time series give insight into the actual dynamics of the network. This will help understand how the brain implements various functions, in particular those involving many circuit feedback loops, such as integrating stimuli with different types of memory to guide behavior<sup>17</sup> and situating the animal in space<sup>9,18</sup>. The method also allows detecting patterns of activity present regardless of a specific stimulus or behavior. Characterizing this spontaneous activity will give further insight into the animal's internal states.

## Methods

### Fly rearing and preparation for imaging

The fly genotype was as described in Supplementary Table 1, and fly stocks were obtained from the Drosophila Bloomington Stock Center. Flies were reared at 25 degrees with a 24 h light/ dark cycle, on brown food (containing cornmeal, molasses, yeast, soy flour, agar, propionate and nipogen) as it had a lower auto-fluorescence than regular yellow food (such as the one from the Bloomington Stock Center that contains yellow cornmeal, malt extract, corn syrup, yeast, soy flour, agar and propionic acid).

Fly holders were 3D printed in black ABS (ordered from ZoomRP with Supplementary data chamberb.stl). A piece of tape (Scotch 3M 0.75" Width) was shaped as a 1 mm high step -using a 1 mm thick glass slide-, and an aperture as in Supplementary Figure 1 (1mm wide for the body and 0.6 mm wide for the head) was made by hand using a sharpened scalpel or a thin lancet (36 gauge, tiniBoy). The tape was then stuck onto the chamber, aligning the hole of the tape to the center of the holder. To block the excitation light from hitting the fly's eyes, black nail polish (Black Onyx nail laquer, OPI products) was added onto the tape. Nail polish was also added at the contact between the tape and the holder to avoid leaks.

Flies were transferred to an empty glass vial and left on ice for approximately one minute. The holder was put in contact with wet tissues on ice under a binocular microscope. A fly from the cold vial was pushed into the holder's hole so as to have the posterior part of the head well centered and in contact with the tape. UV-curing glue (Fotoplast gel, Dreve), was added at the junction between the tape and the head between the eyes and cured for five seconds using a 365 nm Thorlabs LED at 20% of power for 5 seconds. A piece of thin copper wire (Wire-Magnet, 40 Gauge, AmplifiedParts) was added above the legs to push them away from the proboscis (see Supplementary Figure 1) and fixed with UV glue. UV glue was then added at the rim of the eye and all around the proboscis, without touching the antenna or the legs, and cured for 5 seconds. Uncured glue was carefully removed with tissues. The holder was then removed from ice and cleaned again to remove humidity and any trace of remaining glue, and UV light was shone onto the head one last time to make sure that all the glue was cured. The wire was then removed, and a small piece of tissue or a small styrofoam ball was given to the fly to walk on so as to monitor its health during the following steps.

The holder was turned over and the fly's thorax was pushed down to clear the way to the back of the brain. Small pieces of tape were added onto any remaining holes around the fly's body, and UV glue was added on top of them and cured around the thorax to fix it in place. Some glue was then pushed towards the neck with a very thin lancet needle (extracted from 36 Gauge tinyBoy lancets) and cured. Saline (108 mM NaCl, 5 mM KCl, 3 mM CaCl<sub>2</sub>, 4 mM MgCl<sub>2</sub>, 4 mM NaHCO<sub>3</sub>, 1 mM NaH<sub>2</sub>PO<sub>4</sub>, 5 mM trehalose, 10mM sucrose, 5 mM HEPES adjusted to pH 3.5 +/- 0.5 with NaOH, prepared weekly) was added and left for few minutes to make sure that there were no leaks.

Fresh saline was added and dissection was started with forceps (5SF, Dumont) that were priorly sharpened as finely as possible by hand. The cuticle in the middle of the back of the head was first removed, while being careful to cut pieces completely before pulling them out. This exposed the hole in the middle of the brain where muscle 16 resides. The pulsatile piece was pulled out. Fresh saline was added and the remaining of the cuticle was removed piece by piece. Glue was also gently scrubbed away if necessary. The brain was washed with saline several times to remove fat bodies. The air sacks were

then removed very carefully to avoid displacing the brain. After a new wash with saline, the fly was ready for imaging.

### **Imaging set up**

The microscope was modified from an upright Olympus BX51W, with a 20x NA 1.0 XLUMPlanFL objective (Olympus). A microlens array (pitch= 125microns, f/10 to match the objective<sup>2</sup>) ordered from RPC Photonics, was positioned at the image plane using a custom made holder (with some parts from Bioimaging Solutions, Inc). 2 relay lenses (50mm f/1.4 NIKKOR-S Auto, Nikon) projected the image onto the sensor of scientific CMOS camera (Hamamatsu ORCA-Flash 4.0). A 490nm LED (pE100 CoolLED) at approximately 10% of its full power was used for excitation. We used 482/25 bandpass filter, 495 nm dichroic beam splitter and a 520/35 bandpass emission filter (BrightLine, Semrock) for the fluorescence.

The resolution as a function of depth (see Supplementary Figure 1) was determined by imaging 2 microns fluorescent beads dispersed in an agarose gel. After reconstruction, the center of beads at different distance to the focal plane was recorded using ImageJ, and a Matlab program measured the point spread function half height and half width.

The fly holder was positioned on a U shaped stage above a floating ball so that the fly could walk (see Figure 1 and Supplementary Videos 2 and 3). The ball was either a polyurethane foam ball (10 mm in diameter), a styrofoam ball, or a hollow HDPE ball (¼ inch). A cup matching the ball diameter and with a 1.2 mm hole was prepared using self-curing rubber (Sugru). A bottle of compressed air provided a steady flow in a pipeline consisting of a tube and a pipette tip connecting to the cup hole. A micromanipulator (Narishige) allowed to position the ball under the fly's legs. The fly and the ball were illuminated by a row of IR LEDs (940nm, RaspberryPiCafe<sup>®</sup>) in the front and the back of the fly, and were observed at 100 Hz using a small camera (FFMV-03M2M, Point Grey).

For the odor stimulus, air was delivered by a pump (ActiveAQUA AAPA7.8L) through an electrically controlled valve (12 Vdc Normally Closed Solenoid Valve, American Science & Surplus), bubbled in 50% ethanol or 50% apple cider vinegar in a vial, and blown towards the fly through an inverted 1mL pipette tip. The valve circuit was controlled by a relay (RELAY TELECOM DPDT 2A 4.5V, Digi-Key), connected to a labjack U3-HV through a LJTICK-RelayDriver (LabJack). The excitation light and a 365nm or 470nm LED (Thorlabs) for visual stimulation, were also triggered by the LabJack, which was controlled using Matlab programs. In a typical experiment, the cameras for monitoring the behavior and the fluorescence were started first, and then the Matlab program was launched. The fluorescence images were recorded with HCLImage (Hamamatsu) and streamed to RAM on a 64Gb of RAM computer, which allowed to record approximately 1 min of experiment continuously.

### **Analysis**

The movies of the behavior were analyzed manually (pressing different keyboard keys when different behavior were recognized) using a Matlab GUI.

The light field images were reconstructed using a program in python as described in<sup>2</sup>. Briefly, a point spread function library corresponding to the specific set up was first generated. Then the images were reconstructed using 3D deconvolution on a cluster of GPUs (either generously lent by the Calit2

Institute, or purchased from Amazon Web Services). A 10000 time steps dataset took approximately 8 hours to reconstruct on a cluster of 15 GPUs.

The images were assembled in a Nifti file using a routine in python, and the 5 first seconds were discarded as the strong activity in response to the excitation light made it difficult to correct for movement and photobleaching. The 3D image registration function `3dvolreg1` function from AFNI was then used to correct for movements in 3D. The background fluorescence as well as intensity decrease from photobleaching were removed by subtracting a signal smoothed using a box average over 7s. The time series were then multiplied by -1 for Arclight data. Although components could be extracted with unfiltered data, the number of components detected and the clarity of the maps were improved when denoising the data first. A Kalman filter with a gain of 0.5 was better than a median filter over 3 points, and was used for the figures in this paper.

Dimension was then reduced by separating the volumes in slices of thickness corresponding to the point spread function half height, and averaging in z for each slice. Note that some information was lost at this stage as the point spread function half height is larger than Nyquist sampling. However this reduction didn't have a strong effect on further detection of the components in our hands, and sped up the analysis. The 4D data sets were typically 200x100x10x10000 at this stage.

PCA and ICA were applied either with a Matlab code using a distributed SVD algorithm and `Fastica1` or using the melodic function<sup>8</sup> from the FSL package. Melodic gave typically slightly more components and clearer maps so we used it for the figures in this paper. The components were then sorted by hand using a custom made interactive ipython notebook. Only the components for which the maps had recognizable brain structures, or for which the time series showed recognizable patterns of activity such as spikes were kept. The number of components was chosen to have approximately 50% of such components. The other components likely corresponded to movement artefacts or noise, and imposing more components for PCA and ICA typically increased the number of noise components without affecting the components corresponding to brain activity.

### **Image manipulations**

Figure 1b bar was added with imageJ and the 3d rendering was done in `Icy2`, in which transparency and contrast were adjusted globally on the volume. This experiment corresponds to the experiment reported in Figure 3. For Figure 2a, b, and c, and Figure 3, images were zscored at  $2 \times \sigma$  in python (see the ipython notebooks), and only the positive part of the map is displayed. The images contrast was then adjusted globally in imageJ and the figures were assembled in Inkscape.

### **Acknowledgements**

We thank Jürgen Schulze, Joseph Keefe and Calit2 for generously providing a GPU cluster, Charles F. Stevens and Terrence Sejnowski for helpful discussions and comments on the manuscript, and Stephen M. Smith for help with melodic.

1. Lemon, W. C. *et al.* Whole-central nervous system functional imaging in larval *Drosophila*. *Nat Commun* **6**, (2015).
2. Broxton, M. *et al.* Wave optics theory and 3-D deconvolution for the light field microscope. *Opt. Express* **21**, 25418–39 (2013).
3. Prevedel, R. *et al.* Simultaneous whole-animal 3D imaging of neuronal activity using light-field microscopy. *Nat. Methods* **11**, 727–30 (2014).
4. Levoy, M., Ng, R., Adams, A., Footer, M. & Horowitz, M. Light field microscopy. *ACM Trans. Graph.* **25**, 924 (2006).
5. Grosenick, L., Anderson, T. & Smith, S. J. Elastic Source Selection for in vivo imaging of neuronal ensembles. in *Proceedings IEEE International Symposium on Biomedical Imaging: From nano to macro* 6–9 (2009). doi:10.1109/ISBI.2009.5193292
6. Chen, T.-W. *et al.* Ultrasensitive fluorescent proteins for imaging neuronal activity. *Nature* **499**, 295–300 (2013).
7. Jin, L. *et al.* Single action potentials and subthreshold electrical events imaged in neurons with a fluorescent protein voltage probe. *Neuron* **75**, 779–85 (2012).
8. Beckmann, C. F. & Smith, S. M. Probabilistic independent component analysis for functional magnetic resonance imaging. *IEEE Trans. Med. Imaging* **23**, 137–52 (2004).
9. Mukamel, E. A., Nimmerjahn, A. & Schnitzer, M. J. Automated analysis of cellular signals from large-scale calcium imaging data. *Neuron* **63**, 747–760 (2009).
10. Lin, C. Y. *et al.* A Comprehensive Wiring Diagram of the Protocerebral Bridge for Visual Information Processing in the *Drosophila* Brain. *Cell Rep.* **3**, 1739–1753 (2013).
11. Chiang, A.-S. *et al.* Three-dimensional reconstruction of brain-wide wiring networks in *Drosophila* at single-cell resolution. *Curr. Biol.* **21**, 1–11 (2011).
12. Milyaev, N. *et al.* The virtual fly brain browser and query interface. *Bioinformatics* **28**, 411–415 (2012).
13. Aso, Y. *et al.* The neuronal architecture of the mushroom body provides a logic for associative learning. *Elife* **3**, 1–48 (2014).
14. Wilson, R. I. Early olfactory processing in *Drosophila*: mechanisms and principles. *Annu. Rev. Neurosci.* **36**, 217–41 (2013).
15. Behnia, R., Clark, D. A., Carter, A. G., Clandinin, T. R. & Desplan, C. Processing properties of ON and OFF pathways for *Drosophila* motion detection. *Nature* **512**, 427–30 (2014).
16. Gouwens, N. W. & Wilson, R. I. Signal propagation in *Drosophila* central neurons. *J. Neurosci.* **29**, 6239–49 (2009).
17. Seelig, J. D. & Jayaraman, V. Neural dynamics for landmark orientation and angular path integration. *Nature* **521**, 186–191 (2015).
18. Cox, R. W. & Jesmanowicz, a. Real-time 3D image registration for functional MRI. *Magn. Reson. Med.* **42**, 1014–1018 (1999).
19. Hyvärinen, A. Fast and robust fixed-point algorithms for independent component analysis. *IEEE Trans. Neural Netw.* **10**, 626–34 (1999).
20. de Chaumont, F. *et al.* Icy: an open bioimage informatics platform for extended reproducible research. *Nat. Methods* **9**, 690–6 (2012).

Figure 1: Imaging the fly brain using light field microscopy. a) Experimental set up. The fly is head fixed and its tarsi are touching a ball. The light from the brain goes through the objective, the microscope tube lens, a microlens array, and relay lenses, onto the sensor of a high speed sCMOS camera. The behavior is recorded with another camera in front of the fly. b) Example of a light field deconvolution. Top: 2D light field image acquired in 5 ms exposure with a 20x objective. Bottom: Anterior and posterior views (slightly tilted sideways) of the computationally reconstructed volume. 3D bar is 90x30x30 microns.

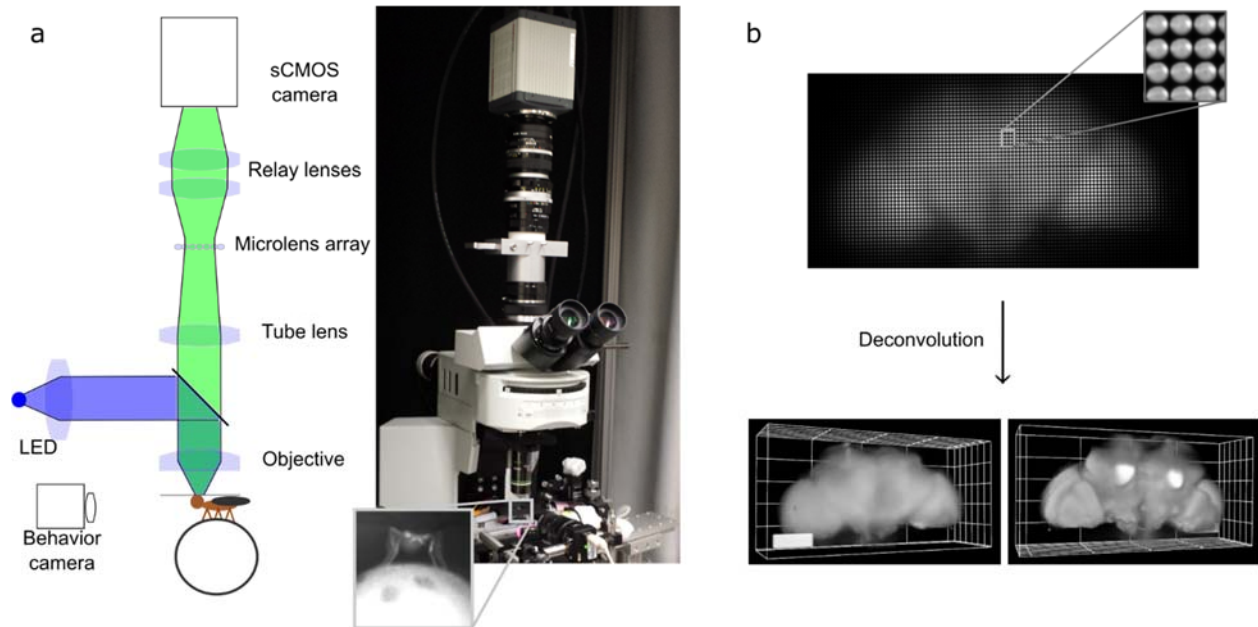




Figure 2: Z-scored thresholded maps and time series of the sources extracted using PCA and ICA. a) Z-stack of the maps obtained when flashes of UV light were presented a fly expressing GCaMP6f pan-neuronally. b) Comparison between functional and anatomical maps. Left: functional maps chosen from figure 2b, S2a and S2b. Right: corresponding anatomical structures. Top three other images corresponding to central complex structures--modified from Cell Reports, Vol. 3, Lin, C. Y. et al., "A Comprehensive Wiring Diagram of the Protocerebral Bridge for Visual Information Processing in the *Drosophila* Brain," 1739-1753, Copyright 2013, with permission from Elsevier--, and four bottom images were generated choosing neurons from the Virtual Fly Brain database. c) Time series (left) associated with the maps (right) sorted by brain regions for the same experiment as a). d) Components extracted from whole brain voltage activity. The fly was presented periodic flashes of UV light (violet bars below) and puffs of apple cider vinegar (pink bars below). Shown on the left are the component time series, while on the right are the corresponding maps (bottom: optic lobe components, middle: antennal lobe, calix, lateral horn and superior medial protocerebrum components, top: central complex components). Bar: 90 microns.

